A Proteomic Survey Indicates Sortilin as a Secondary Substrate of the ER Translocation Inhibitor Cyclotriazadisulfonamide (CADA)*[S]

Victor Van Puyenbroeck‡¶, Elisa Claeys‡¶, Dominique Schols‡, Thomas W. Bell§, and Kurt Vermeire‡‖

The small molecule CADA was shown to down-modulate the expression of human CD4 in a signal peptide-dependent way through inhibition of its cotranslational translocation across the ER membrane. Previous studies characterizing general glycoprotein levels and the expression of 14 different cell surface receptors showed selectivity of CADA for human CD4. Here, a PowerBlot Western Array was used as a screen to analyze the proteome of CADA-treated SUP-T1 human CD4$^+$ T lymphocytes. This high-throughput monoclonal antibody panel-based immunoblotting assay of cellular signaling proteins revealed that only a small subset of the 444 detected proteins was differentially expressed after treatment with CADA. Validation of these proteomic data with optimized immunoblot analysis confirmed the CADA-induced change in expression of the cell cycle progression regulator pRb2 and the transcription factor c-Jun. However, the up-regulation of pRb2 or down-modulation of c-Jun by CADA had no impact on cell cycle transition. Also, the reduced protein level of human CD4 did not inhibit T cell receptor signaling. Interestingly, the signal peptide-containing membrane protein sortilin was identified as a new substrate for CADA. Both cellular expression and *in vitro* cotranslational translocation of sortilin were significantly reduced by CADA, although to a lesser extent as compared with human CD4. Our data demonstrate that a small signal peptide-binding drug is able to down-modulate the expression of human CD4 and sortilin, apparently with low impact on the cellular proteome. ***Molecular & Cellular Proteomics 16: 10.1074/mcp.M116.061051, 157–167, 2017.***

According to the World Health Organization, the human immunodeficiency virus (HIV) has infected almost 78 million people worldwide since its discovery in the early eighties, resulting in the death of more than 34 million people. Currently, 25 different Food and Drug Administration-approved anti-HIV drugs are in clinical use, turning HIV and acquired immune deficiency syndrome into a more chronic disease, yet not curable. In addition, HIV can develop resistance to almost all classes of antiretroviral drugs, making the development of new therapies and anti-HIV drugs an ongoing challenge (1).

The synthetic small molecule cyclotriazadisulfonamide (CADA;[1] Fig. 1*A*) was identified as a novel anti-HIV agent in an earlier screening program (2). This compound prevents viral entry of different HIV-1 lab strains and clinical isolates into T lymphocytes but does not interact with viral components. Instead, CADA down-modulates the cell surface expression of the human CD4 (hCD4) glycoprotein (2–7), known as the main receptor for HIV entry (8). Moreover, a strict correlation between the hCD4 down-modulating activity and anti-HIV potency of CADA-derived compounds has been demonstrated (3).

Recently, the mechanism of action of CADA has been unraveled: The drug selectively binds to the signal peptide (SP) of the hCD4 preprotein and prevents it from being translocated into the lumen of the endoplasmic reticulum (ER) (9). Signal peptides (also called signal sequences) are located at the amino terminus of preproteins destined for secretion or plasma membrane insertion. They are crucial for targeting those proteins to the secretory pathway (10). Despite their distinct functional role, signal peptides are diverse and lack a conserved primary sequence (11).

Our previous studies showed that hCD4 protein biogenesis is inhibited by CADA in a signal-peptide-dependent way, resulting in a significant down-modulation of cell surface hCD4 levels. They also suggested selectivity of CADA for hCD4 as the compound does not affect cell surface expres-

From the ‡KU Leuven - University of Leuven, Department of Microbiology and Immunology, Rega Institute for Medical Research, Laboratory of Virology and Chemotherapy, B-3000 Leuven, Belgium; §Department of Chemistry, University of Nevada, Reno, NV, USA

Received May 13, 2016, and in revised form, November 4, 2016
Published, MCP Papers in Press, December 20, 2016, DOI 10.1074/mcp.M116.061051
Author contributions: V.V.P., E.C., and K.V. designed the research; V.V.P., E.C., and K.V. performed the research; D.S. and T.W.B. contributed new reagents or analytic tools; V.V.P. and E.C. analyzed data; and V.V.P., E.C., T.W.B., and K.V. wrote the paper.

[1] The abbreviations used are: CADA, cyclotriazadisulfonamide; BD, Becton Dickinson; ER, endoplasmic reticulum; hCD4, human cluster of differentiation 4; HIV, human immunodeficiency virus; LAT, linker for activation of T cells; Lck, leukocyte C-terminal Src kinase; pPL, preprolactin; pRb2, retinoblastoma-like protein 2; SP, signal peptide; TCR ,T cell receptor; Tris, tris(hydroxymethyl)aminomethane; ZAP-70, zeta-chain-associated protein kinase 70.

sion of 14 different T lymphocyte receptors nor CD4 from nonprimate species. In addition, cell lysate analysis with concanavalin A agarose beads demonstrated no changes in the expression of glycosylated membrane proteins other than hCD4 (2, 9).

Here, we employed a PowerBlot™ Western Array to identify potential other substrates of CADA (besides hCD4) in human $CD4^+$ T lymphocytes. This high-throughput immunoblotting technology simultaneously evaluates changes in the expression and posttranslational modification of several hundreds of cellular signaling proteins in total cell extracts from treated and untreated cells. Analysis identified a small subset of the 444 detected proteins as being affected by CADA. Of these, the signal-peptide-containing membrane protein sortilin was validated as a new substrate of CADA.

MATERIALS AND METHODS

Compounds and Antibodies—Cyclotriazadisulfonamide hydrochloride was dissolved in dimethyl sulfoxide (DMSO) to obtain a 10 mM stock solution for use in cell culture. FITC-labeled anti-human CD4 [clone SK3] (BioLegend), phycoerythrin-labeled anti-human CD4 [clone SK3] (BioLegend), and allophycocyanin-labeled anti-human CD4 [clone SK3] (BD Biosciences) monoclonal antibodies were used for flow cytometry. Anti-CD3 [clone OKT3] from eBioscience and goat anti-mouse IgG [Poly4053] from BioLegend were used for TCR activation. Western blotting antibodies were purchased from (i) BD Biosciences: anti-human CD4 [clone SK3], GAP1m [clone 15], p19 skp1 [clone 52], sequestome-1/p62 Lck ligand [clone 3], FUS/TLS [clone 15], XRCC4 [clone 4], p56 Lck [clone 28], Rb2 [clone 10], clathrin [clone 23]; (ii) Thermo Scientific: anti-c-Jun [clone 5B1], STAT1 [clone 15H3], cyclin D3 [clone DCS-22]; (iii) R&D Systems: anti-sortilin [clone 334708]; (iv) Abcam: anti-sortilin [clone EPR15010]; (v) Abnova: anti-ASAP-1 [clone 2G7]; (vi) Dako: HRP-labeled goat anti-mouse immunoglobulins, HRP-labeled swine anti-rabbit immunoglobulins; and (vii) Cell Signaling Technologies: polyclonal anti-LAT, pLAT (Tyr191), pZAP-70 (Tyr493), monoclonal anti ZAP-70 [clone D1C10E], pZAP-70 (Tyr319) [clone 65E4], HRP-labeled goat anti-rabbit immunoglobulins.

Cell Culture—Cells were obtained from the American Type Culture Collection and were maintained at 37 °C with 5% CO_2. SUP-T1, and Jurkat lymphoma cells were cultured in Roswell Park Memorial Institute 1640 medium (Life Technologies) supplemented with 10% fetal bovine serum (HyClone, GE Lifesciences) and 2 mM L-glutamine (Life Technologies). HEK293T cells were cultured in Dulbecco's Modified Eagle Medium (Life Technologies) supplemented with 10% fetal bovine serum, 1 mM sodium pyruvate (Life Technologies), and 0.075% sodium bicarbonate (Life Technologies).

Plasmids—Plasmid pGEMBP1 encoding bovine preprolactin (pPL) has been described previously (12). Inverse PCR-based site-directed mutagenesis (13) was used to replace the pPL signal peptide in pGEMBP1 with the sortilin signal peptide (residues 1–33). The hCD4/pPL chimeric construct and the pcDNA3 expression vector encoding hCD4 have been described (9). The pCMV6-AC-GFP vector containing SORT1 cDNA was obtained from OriGene Technologies.

Flow Cytometry—SUP-T1 cells were seeded at 1.5×10^5 cells/ml in Corning Costar 24-well plates, supplemented with the indicated amount of CADA or 0.1% DMSO as a control and were incubated for 72 h. Cells were then washed in PBS and stained with anti-hCD4-FITC. Samples were stored in PBS containing 1% formaldehyde before acquisition on a FACSCalibur flow cytometer (BD Biosciences) with BD CellQuest software v3.3. A FACS Canto II flow cytometer (Becton Dickinson) with BD FACSDiva 8.0.1 software was used for cell cycle analysis and to quantify expression of hCD4 (stained with phycoerythrin-labeled anti-hCD4) on SUP-T1 and Jurkat cells after T cell receptor activation. Transfected HEK293T cells were collected 48 h after transfection. Sortilin expression was determined through GFP fluorescence, and hCD4 expression was measured with anti-hCD4-APC on a FACSCanto II flow cytometer. All flow cytometric data were analyzed in FlowJo v10.1.

BD PowerBlot™ Western Array—Cells were left untreated or were treated with 16 μM CADA for 72 h before lysis in boiling lysis buffer (10 mM tris(hydroxymethyl)aminomethane (Tris)·HCl pH 7.4, 1 mM sodium orthovanadate, and 1% sodium dodecyl sulfate (SDS)). Lysates were homogenized by sonication and total protein concentration was determined with the bicinchoninic acid protein assay (Pierce) before freezing at −80 °C for shipping to BD Biosciences on dry ice. Protein (200 μg) was loaded in one big lane across the entire width of a 130 × 100 × 0.5 mm, 4–15% SDS-polyacrylamide gel. Electrophoresis was performed at 150 V for 90 min, and the proteins were wet-transferred to Immobilon-P membranes (Millipore). After transfer, the membranes were dried and rewet in methanol before incubation with blocking buffer (LI-COR) for 1 h. A manifold that isolates 41 narrow channels was clamped to the membrane, and a complex antibody mixture was added to each channel. In this way, a panel of 1000 different monoclonal antibodies was hybridized across five identical membranes. After 1 h incubation, the blot was removed from the manifold, washed, and hybridized for 30 min with goat anti-mouse conjugated to Alexa Fluor 680 (Molecular Probes). Then, the membrane was washed, dried, and scanned at 700 nm on an Odyssey Infrared Imaging System (LI-COR). Lanes 40 or 41 were incubated with an antibody mixture detecting molecular weight standards. Signal intensities from each spot were quantified, normalized, and expressed as a ratio to determine increase or decrease in protein expression. Normalization was done by multiplying the raw signal intensity of a spot by 1×10^6 and dividing by the total signal intensity of all valid spots on an image. Triplicate blots for control and treated were compared in a 3 × 3 matrix, *e.g.* control run 1 was compared with treated run 1, 2, and 3; control run 2 was compared with treated run 1, 2, and 3, etc. The resulting nine comparisons were used for the determination of a semi-quantitative fold change value. Signals with a greater than 1.25-fold change were classified based on the size of change, signal quality, and visual inspection of signal spots by a technician. 10 confidence levels were used for classification (Table S1), with 10 being the highest level of confidence.

Bioinformatic Tools—To identify proteins with a signal peptide or uncleaved signal anchor sequence, we analyzed protein reference sequences obtained from the UniProt database (http://www.uniprot.org/uniprot/) with SignalP v4.1 (http://www.cbs.dtu.dk/services/SignalP/), TargetP v1.1 (http://www.cbs.dtu.dk/services/TargetP/), TMHMM v.2.0 (http://www.cbs.dtu.dk/services/TMHMM/) (14), and Phobius (http://phobius.cgb.ki.se/) (15). Results were validated against the curated UniProtKB database annotation.

Classical Western Blotting—SUP-T1 cells were seeded at 1.5×10^5 cells/ml and treated with 10 μM CADA or 0.1% DMSO as a control for 72 h. To detect hCD4, the cells were lysed in ice-cold Nonidet P-40 buffer [50 mM Tris·HCl (pH 8.0), 150 mM NaCl, 1% Nonidet P-40] supplemented with protease inhibitor mixture (Roche) and centrifuged at 14.000 × *g* for 10 min to pellet nuclei and debris. All other proteins were extracted by lysing cells in ice-cold radioimmunoprecipitation assay buffer [50 mM Tris·HCl (pH 8.0), 150 mM NaCl, 1% Nonidet P-40, 1% sodium deoxycholate, 0.5% SDS] and homogenized by passing the samples 10 times through a 26-gauge needle. Total protein concentration of all samples was determined with the bicinchoninic acid protein assay (Pierce). For SDS gel electrophoresis, samples were boiled in reducing 2X Laemmli sample buffer [120 mM Tris·HCl (pH 6.8), 4% SDS, 20% glycerol, 100 mM dithiothreitol,

0.02% bromphenol blue]. Nonreducing buffer lacking dithiothreitol was used for the hCD4 lysates. Equal protein amounts (~8 μg per lane, equivalent to the PowerBlot concentration) were separated on 4–12% Criterion XT Bis-Tris gels (Bio-Rad) using MES buffer (Bio-Rad). After electrophoresis, gels were blotted onto PVDF membranes using the Trans-Blot Turbo transfer system (Bio-Rad). Membranes were blocked for 1 h with 5% nonfat dried milk in TBST (20 mM Tris·HCl (pH 7.6), 137 mM NaCl, 0.05% Tween-20). After overnight incubation of the primary antibodies at 4 °C, membranes were washed and incubated with the secondary antibodies. SuperSignal West Femto chemiluminescence reagent (Pierce) was used for detection in conjunction with a ChemiDoc MP system (Bio-Rad), and signal intensities were quantified with Image Lab software v5.0 (Bio-Rad). Differences in protein concentration between each lane were compensated by normalizing for the clathrin heavy chain signal.

T Cell Receptor Stimulation—Jurkat or SUP-T1 cells were seeded in RPMI1640 medium supplemented with 10% FBS, 2 mM L-glutamine, and 10 mM CADA or 0.1% DMSO as a control and incubated for 24 h at 37 °C, 5% CO_2. The cells were washed and placed on ice for binding of mouse anti-CD3 and goat anti-mouse IgG antibodies. TCR signaling was then activated by placing the cells in a 37 °C water bath for 2 min, followed by immediate cooling and lysis in Nonidet P-40 buffer (50 mM Tris-HCl (pH 8.0), 150 mM NaCl, 1% Nonidet P-40, 0.5 mM PMSF) supplemented with cOmplete protease inhibitor mixture (Roche) and phosphatase inhibitor mixture (Active Motif). Lysates were cleared by centrifugation (15 min at 17,000 × *g* and 4 °C), and the supernatant was boiled in 2X reducing Laemmli sample buffer for SDS-PAGE and Western blotting analysis (described above).

Cell Cycle Analysis—SUP-T1 cells were seeded in Corning Costar 24-well plates at 1.5×10^5 cells/ml, supplemented with 0.1 nM to 1 μM palbociclib (PD-0332991, Sigma), 10 μM CADA or 0.1% DMSO as a control and incubated for 48 h at 37 °C with 5% CO_2. Next, cells were washed with ice-cold PBS and fixed in ice-cold methanol. Cells were then washed again and stained with 10 μg/ml propidium iodide and 50 μg/ml RNase A for flow cytometric analysis.

Cell Transfection—HEK293T cells were plated at 3×10^5 cells/ml in Corning Costar 24-well plates and were transfected with human SORT1 and/or hCD4 plasmid cDNA 24 h after plating. Transfections were carried out by making use of Lipofectamine 2000 transfection reagent (Invitrogen). After 6 h, indicated amounts of CADA or 0.1% DMSO were added, and cells were collected for flow cytometric analysis 48 h after transfection.

Cell-free In Vitro Translation—Full-length mRNAs were transcribed *in vitro* from NheI linearized pGEM plasmids using T7 RNA polymerase (RiboMAX system, Promega) and translated in rabbit reticulocyte lysate (Promega) in the presence of L-[^{35}S]-methionine (Perkin Elmer). Translations were performed at 25 °C for 45 min in the presence or absence of sheep pancreatic microsomes. The proteinase K (Roche) digestion was performed on ice for 30 min and quenched with phenylmethylsulfonyl fluoride (Thermo Fisher Scientific). 10 μl reaction mixtures were diluted with 300 μl low-salt buffer (80 mM KOAc, 2 mM $Mg(OAc)_2$, 50 mM HEPES, pH 7.6), and radiolabeled proteins were centrifuged for 10 min at 21,382 × *g* and 4 °C (Hettich 200R centrifuge with 2424-B rotor). Supernatant was removed, and the pellet was resuspended in 30 μl Laemmli sample buffer. The radiolabeled proteins were then separated by SDS-PAGE, dried, and analyzed with a Cyclone Plus phosphor imager system (Perkin Elmer).

Experimental Design and Statistical Rationale—For each flow cytometric sample, 5000 to 20,000 cells were analyzed, and at least two biological replicates were performed, as indicated in the figure legends. The BD PowerBlot™ used a single control and treated sample set, with three technical repeats that were compared in a 3 × 3 matrix. The subsequent validation experiments were also based on a single set of control and treated sample, and four technical repeats were performed to obtain a reasonable estimate of the mean fold change. For a protein with equal expression level in control and CADA-treated cells, the ratio of signals in control and CADA-treated cells will be 1. We employed a one-way analysis of variance with Dunnett's post hoc test to evaluate whether the log2-transformed ratios in our validation were significantly different from 1. To control the false positive rate of the entire family of comparisons, *p* values were adjusted to take into account that multiple comparison tests are conducted. The multiplicity adjusted *p* value of a particular hypothesis is defined as the smallest significant level, when applied to the entire family of hypotheses, at which this particular hypothesis will be deemed statistically significant. The familywise significance level was set to 5% for all experiments. All statistics were done in GraphPad Prism v7.0.

RESULTS

Use of the PowerBlot™ Western Array for Proteomic Analysis of CADA-Treated SUP-T1 Cells—In an earlier study, we demonstrated how the small molecule CADA down-modulates hCD4 receptor expression by selective binding to the hCD4 preprotein signal peptide with subsequent cotranslational translocation inhibition (9). To further investigate the substrate selectivity of this drug, a proteomic study was set up in the human $CD4^+$ T cell lymphoma SUP-T1. Cells were left untreated or were exposed to CADA for 72 h. The hCD4 down-modulating activity of CADA in our samples was verified by flow cytometry (Fig. 1*B*), before further downstream analysis with a PowerBlot™ Western Array (BD Biosciences).

A panel of 1000 different monoclonal antibodies targeting a wide range of cellular signaling proteins was used in the array; 574 antibodies returned a detectable signal in the PowerBlot samples of SUP-T1 cells (Table S2), which mapped to 444 unique proteins (for several proteins multiple antibodies were used to identify different posttranslational modifications).

In the standard PowerBlot antibody panel, anti-hCD4 was not originally included. In order to detect our control protein, an anti-hCD4 antibody from BD (validated for flow cytometry only) was added to the antibody mixture. Unfortunately, the generalized multitarget Western blotting settings did not allow detection of hCD4 in the PowerBlot screening (Fig. S1, last two lanes), even though flow cytometry data had confirmed the presence of hCD4 in SUP-T1 cells and its down-modulation by CADA (Fig. 1*B*). Protein samples in the PowerBlot assay were separated on a reducing SDS-PAGE, but nonreducing conditions have been reported for immunoblotting of hCD4 (16, 17). As expected, hCD4—which contains four immunoglobulin-like extracellular domains, three of them stabilized by disulfide-bridges (18)—could be clearly detected when nonreducing conditions were used for sample preparation and SDS-PAGE (Fig. 1*C*). Moreover, the Western blotting data show how CADA treatment results in a dose-dependent reduction of total hCD4 protein expression, which was identical to the flow cytometric analysis of cell surface hCD4 (Fig. 1*D*).

Analysis of the SUP-T1 PowerBlot Suggests Several Potential CADA Targets—When all confidence levels were taken into account in the PowerBlot analysis, 54 of the 574 detected

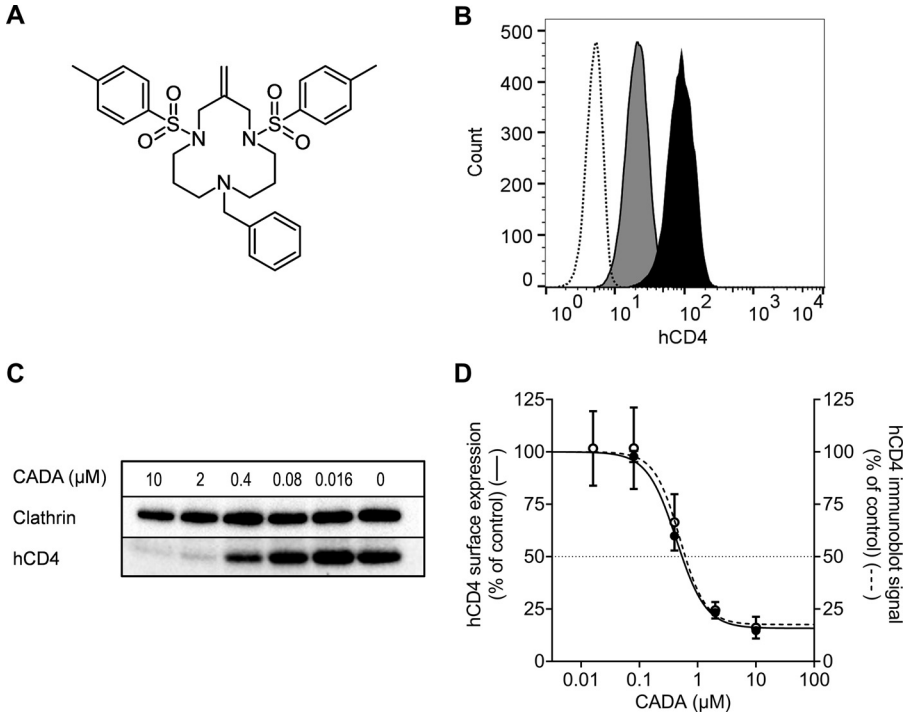

FIG. 1. **CADA dose-dependently down-modulates surface hCD4 expression.** (*A*) Structure of cyclotriazadisulfonamide (*CADA*). (*B*) Flow cytometric determination of the hCD4 surface expression on SUP-T1 cells after 72 h treatment with 16 μM CADA, to verify hCD4 down-modulation by CADA in the samples subjected to PowerBlot™ analysis. Dotted line: unstained control; black: untreated control; gray: CADA. (*C*) After 72 h treatment of SUP-T1 cells with CADA, hCD4 was detected with Western blotting under nonreducing conditions. One representative blot out of four is shown. (*D*) Flow cytometric analysis of the hCD4 surface expression level before lysis (left axis, solid line, mean ± S.E., $n = 5$, absolute $IC_{50} = 0.63$ μM). Total hCD4 protein levels from the immunoblots in (*C*) were quantified and normalized to the clathrin control (right axis, dotted line, mean ± S.E., $n = 4$, absolute $IC_{50} = 0.71$ μM). Absolute IC_{50}: CADA concentration that reduces the hCD4 expression to 50% of the untreated control.

antibody signals were down- or up-regulated by CADA treatment (Tables S2 and S3). We selected several candidate proteins for further analysis and validation. While a traditional approach would use an estimation of the amount of false positives and negatives in the dataset to select appropriate candidates, our target selection was primarily based on the BD's confidence level classification parameters (see Table S1 for a description of the different confidence levels). Fig. 2 shows a comparison between the BD PowerBlot candidates (from all 10 confidence levels) and a more common statistical analysis that uses the false discovery rate approach for candidate selection. The confidence level method used by BD mainly classified proteins located in the upper left and upper right portion of the graph (Fig. 2), which corresponds to the highest change in expression level and lowest risk for false positives. In addition, this classification also considers parameters such as low signal to reduce the amount of false positives in our candidate selection.

We selected the proteins with the highest confidence level for further validation with classical immunoblotting because the expression level of these nine potential CADA substrates was changed more than twofold in CADA-treated samples (Tables I and S2). This approach has also been used in several other PowerBlot studies (19–21). Individual immunoblots were optimized for the detection of each protein, and we chose the abundantly expressed heavy chain of the structural protein clathrin as an internal control (predicted molecular weight of 192 kDa) that could be detected simultaneously with each selected target protein. Representative immunoblots of the nine potential targets are given in Fig. 3*A*. Surprisingly,

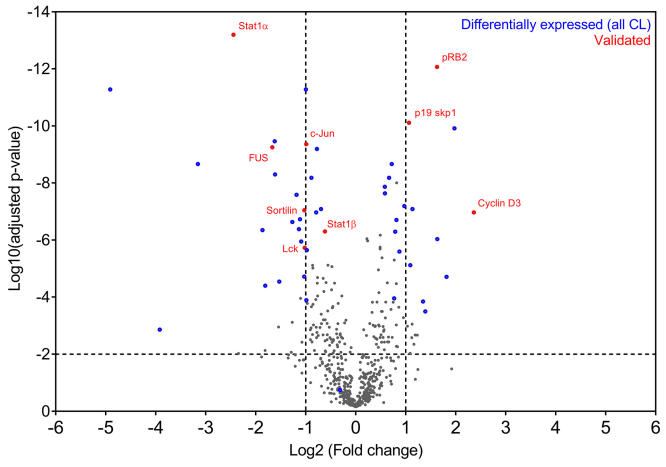

FIG. 2. **PowerBlot confidence-level-based substrate classification is in accordance with false discovery rate target selection.** 574 signals were successfully mapped to the list of BD PowerBlot antibodies and the normalized fold changes (mean of nine replicate measurements for each antibody, see methods) were log2 transformed for further analysis. *p* values were calculated for each set of antibody signals, using an unpaired *t* test without assuming a consistent S.D. We used the false discovery rate approach to adjust the *p* values for multiple comparison testing (two-stage linear step-up procedure of Benjamini, Krieger, and Yekutieli, with Q = 1%), which resulted in 202 signals with an adjusted *p* value <0.01; this threshold is indicated in the volcano plot with a dotted horizontal line. PowerBlot confidence-level-selected substrates are indicated in blue, whereas the targets validated by optimized immunoblots are represented in red.

almost none of the validation immunoblots could confirm a clear effect of CADA on the expression level of these nine proteins (Fig. 3*A*). Retinoblastoma-like protein 2 (pRb2) was

TABLE I
Potential CADA-affected PowerBlot targets selected for validation

Uniprot ID	Protein	Function	CL[a]	Fold change PB[b]	Fold change WB[d]
Q9ULH1	**ASAP1** (Arf-GAP with SH3 domain, ANK repeat and PH domain-containing protein 1)	Regulates ADP-ribosylation factor 1 GTPase activity	10	−n.v.[c]	1.1
Q15283	**GAP1m** (Ras GTPase-activating protein 2)	Inhibitory regulator of Ras cAMP signaling Binds inositol tetrakisphosphate (IP4)	10	−n.v.	1.3
P63208	**p19 skp1** (S-phase kinase-associated protein 1)	Component of the SCF ubiquitin ligase complex	10	−n.v.	1.1
P42224	**STAT1** (Signal transducer and activator of transcription 1)	Signal transducer and transcription activator for interferon and cytokine signaling	10	−5.5	1.2
P35637	**FUS** (RNA-binding protein FUS)	Binds DNA, may act as a transcription activator	10	−3.2	−1.2
Q13426	**XRCC4** (DNA repair protein XRCC4)	Involved in non-homologous end joining DNA repair	10	−n.v.	1.2
P30281	**Cyclin D3** (G1/S-specific cyclin-D3)	Regulates cell cycle progression	10	5.7	1.2
Q13501	**Sequestome-1** (p62 Lck ligand)	Phosphotyrosine-independent ligand for the Lck SH2 domain	10	2.4	1.1
Q08999	**pRb2** (Retinoblastoma-like protein 2)	Regulates cell cycle progression	10	3.1	1.7*
P05412	**c-Jun** (Transcription factor AP-1)	Transcription factor, binds AP-1 and CRE-like sites	9	−2.0	−1.9*
Q99523	**Sortilin** (Neurotensin receptor 3)	Sorting receptor in the Golgi compartment	7	−2.1	−3.8*
P06239	**p56 Lck** (Tyrosine-protein kinase Lck)	CD4/CD8 associated signal transducer for T-cell antigen receptor	3	−2.1	1.2
P01730	**CD4** (cluster of differentiation 4)	MHC class-II antigen/TCR co-receptor	n.v.	n.v.	−8.2*

[a] Confidence level: assigned using signal criteria listed in Table S1.

[b] Mean fold change of the nine comparisons between DMSO and CADA samples in a 3 × 3 matrix as explained in Materials and Methods.

[c] n.v. = no value. See the results section for details on CD4 detection in the PowerBlot system. Presence versus absence of a protein: fold change is not calculable. When no signal could be detected in the CADA (or DMSO) sample but sufficient signal in the corresponding DMSO (or CADA) sample, the difference was classified as > twofold, although no actual ratio could be calculated (number/0).

[d] Mean fold change in four classical Western blots, numbers significantly different from 1 are indicated with (*).

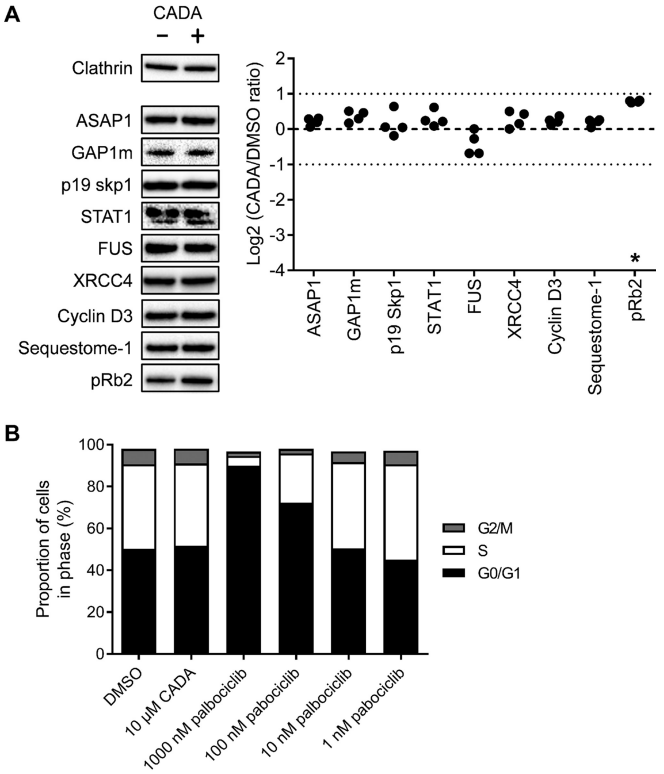

FIG. 3. **Optimized immunoblot validation of BD PowerBlot CL10-assigned targets shows up-regulated pRb2 levels with CADA but cell cycle progression is not affected.** (*A*) DMSO and CADA-treated (10 μM, 72 h) SUP-T1 samples were blotted under reducing conditions. Selected proteins were detected with conditions optimized for each individual primary antibody and representative images are shown for each protein (*left panel*). The signal intensity of the detected proteins in four independent immunoblot experiments were quantified and normalized to the clathrin internal control. The ratio between CADA and control (*DMSO*) signals for each protein is displayed as a Log_2 value (*right panel*). The threshold for twofold change ($Log_2 \pm 1.0$), employed in the BD PowerBlot, is indicated with dotted lines. Star indicates significantly different from untreated control according to one-way ANOVA using Dunnett's post hoc test and a familywise significance level of 5%. (*B*) SUP-T1 cells were grown in the presence of DMSO, CADA or palbociclib for 48 h before staining with propidium iodide and analysis of the cell cycle transition by flow cytometry. Bars in the graph represent mean values, $n = 3$.

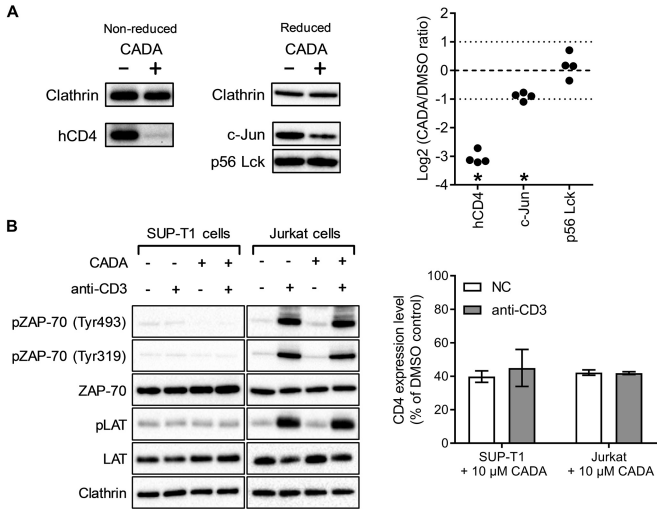

FIG. 4. **CADA down-modulates hCD4 and c-Jun but does not affect phosphorylation events involved in early TCR signaling.** (*A*) DMSO and CADA-treated (10 μM, 72 h) SUP-T1 samples were blotted under nonreducing (*left*) and reducing conditions (*right*). Selected proteins were identified with conditions optimized for each individual primary antibody and representative images are shown for each protein. Quantification was performed as in Fig. 3*A*. (*B*) SUP-T1 and Jurkat cells were grown in the presence of DMSO or CADA (10 μM) for 24 h. Phosphorylation of TCR signaling proteins was then induced through cross-linking of CD3, followed by cell lysis and Western blotting (*left panel*; one representative set of blots out of two experiments is shown). Flow cytometric quantification of surface hCD4 levels on these cells shows that the down-modulation of hCD4 by 24 h CADA-treatment was comparable between SUP-T1 and Jurkat cells, independent of activation by crosslinking CD3 (*right panel*; *bars* are mean ± S.E., $n = 2$).

the only protein with a significant change in expression (1.7-fold). This significant up-regulation of pRb2 correlated well with the PowerBlot analysis (Table I).

As pRb2 is known to regulate G1/S cell cycle transition (22), we next evaluated whether CADA affects cell cycle progression by using propidium iodide staining of CADA-treated SUP-T1 cells and flow cytometry. The small molecule palbociclib is a selective inhibitor of cyclin dependent kinase 4 and 6 (Cdk4/D IC_{50} = 11 nM) (23) and was used as a control for G1/S arrest. Fig. 3*B* shows how palbociclib causes a clear accumulation of SUP-T1 cells in the G0/G1 phase and a reduction of the S and G2/M populations at concentrations ≥100 nM. CADA however, had no effect on the cell cycle distribution, as compared with the DMSO-treated control (Fig. 3*B*).

CADA Additionally Down-Modulates an Intracellular hCD4-Related Signaling Protein—To expand the selection of other candidate CADA-targets for further investigation, we next focused on hCD4-related proteins. hCD4 acts as a coreceptor for the T cell receptor (TCR)-CD3 complex on T-helper immune cells, which recognizes peptides presented on the major histocompatibility complex II. Lck (leukocyte C-terminal Src kinase) is a T-cell-specific protein tyrosine kinase that is constitutively associated with the cytoplasmic C terminus of CD4 and CD8 membrane proteins and acts in the TCR signaling cascade (24). The transcription factor c-Jun is part of the AP-1 activation complex and can be induced by the JNK pathway, which in turn can be activated through CD4 signaling (25). Despite the lower confidence level of Lck and c-Jun in the PowerBlot analysis (Table I), we selected these candidate proteins for validation by optimized immunoblots. As shown in Fig. 4*A*, we measured a significant decrease in the expression of hCD4 (8.2-fold), and c-Jun (1.9-fold). Cell cycle progression is also the main function of c-Jun, but as described above, cell cycle transition was not affected by CADA (Fig. 3*B*).

As CADA-treatment reduces the amount of cell surface hCD4, it may have a potential impact on hCD4 receptor signaling in T cells. We therefore examined whether phosphorylation of several signaling components in the TCR signaling pathway of CD4-positive T cells is affected by CADA. Activation of the TCR-CD3 complex triggers a signaling cascade, which is required for the *in vivo* proliferation and differentiation of T cells. Early signaling involves phosphorylation of the zeta-chain-associated protein kinase 70 (ZAP-70). Tyr493 is phosphorylated by the activated TCR-CD3 complex and activates the enzymatic activity of ZAP-70. Importantly, the hCD4-associated tyrosine kinase Lck can phosphorylate Tyr319 in ZAP-70, which is also important for signaling (26). Phosphorylated ZAP-70 will then activate downstream targets such as linker for activation of T cells, an essential protein in branching of the TCR signaling response (27).

To verify TCR signaling in CADA-treated cells, we stimulated T cells through antibody-mediated cross-linking of the TCR-CD3 complex and then measured the phosphorylation state of ZAP-70 and LAT with Western blotting (Fig. 4*B*). Although described as a very robust method for T cell activation, the amount of phosphorylated ZAP-70 and LAT was not increased in stimulated SUP-T1 cells. We therefore performed an analog experiment with Jurkat cells, a T cell line that has been used extensively in TCR signaling research (28). As shown in Fig. 4*B*, antibody-mediated stimulation of Jurkat cells causes strong phosphorylation of the signaling proteins, which was similar in CADA-treated cells.

CADA Inhibits the Cotranslational Translocation of Sortilin into the ER Lumen—Finally, as CADA inhibits the cotranslational translocation of hCD4 (9), we searched for other proteins that utilize the same ER-targeting pathway. We used bioinformatic prediction tools and the reviewed UniProtKB annotation of the antibody targets to determine that five of the proteins detected in the PowerBlot contained a noncleavable signal anchor sequence, and 22 proteins contained an SP (Table S4). Three of these SP-carrying proteins were classified by PowerBlot as differentially expressed: sortilin, cathepsin D, and semaphorin-4D. However, sortilin was the only protein that passed visual inspection of the PowerBlot antibody signal and was allocated confidence level 7 (Table S3). Furthermore, sortilin was also down-modulated by CADA, whereas for cathepsin D and semaphorin-4D an up-regulation was observed. As evidenced by optimized immunoblots for sortilin (Table I), we validated this protein as a significantly down-modulated target of CADA (3.8-fold). However, the down-modulating effect of CADA on sortilin was only half of that on hCD4.

Next, we determined whether both sortilin and hCD4 receptors are comparable substrates of our compound. Sortilin, also known as neurotensin receptor 3, shuttles between the cell surface and various organelles but is mainly expressed on the membranes of intracellular compartments such as the ER, Golgi, and endosomes. It is a sorting receptor that is involved in protein sorting and targeting of ligands toward endosomes and lysosomes (29, 30). Because no monoclonal antibodies were available for intracellular detection of sortilin by flow cytometry, we obtained a plasmid encoding for GFP-fused sortilin so that sortilin expression could be determined by fluorescence of its GFP tag. To compare sortilin with hCD4 levels, HEK293T cells were cotransfected with sortilin-GFP and wild-type hCD4 encoding plasmids, and expression of both proteins was detected simultaneously with flow cytometry. As shown in Fig. 5*A*, CADA down-modulated sortilin by about 50% but had a much stronger impact on hCD4 levels. Similar down-modulation of sortilin by CADA was also observed when cells were transfected with sortilin-GFP alone (data not shown), excluding competition between the two substrates. Accordingly, immunoblotting of CADA-treated SUP-T1 samples for sortilin revealed a dose–response effect of CADA on the protein level of wild-type sortilin (Fig. 5*B*). Similar results were obtained with another sortilin antibody (data not shown).

Finally, to address whether CADA also down-modulates sortilin in a signal peptide-dependent way, we tested the impact of CADA on protein translocation in a cell-free *in vitro* translation system similar to that used in an earlier study on hCD4 (9). The signal peptide of sortilin was fused to the mature protein of bovine preprolactin (pPL) as outlined in Fig. 5*C*. Wild-type pPL and an hCD4-PL chimera were included as controls. Whereas CADA had little impact on the translocation of wild-type pPL, it partially prevented the translocation of PL when this protein contained the SP of sortilin (Fig. 5*C*, about 50% inhibition at 15 μM CADA). This indicates that the observed susceptibility of sortilin to CADA resides in its N-terminal SP. Moreover, exchanging the SP of pPL for the N-terminal SP-containing region of hCD4 rendered PL fully susceptible to the translocation inhibitory effect of CADA (Fig. 5*C*, 87% inhibition at 15 μM CADA).

DISCUSSION

In this study, we investigated whether there are additional substrates for the small molecule CADA besides hCD4. Only a limited selection of surface receptors was evaluated in previous work (2, 9), and we have now used Western array immunoblotting technology to perform a proteomic survey. Our current screen in the human $CD4^+$ T cell lymphoma SUP-T1 was based on a panel of 1000 monoclonal antibodies covering the whole spectrum of intracellular pathways and categories related to cell division, cell signaling, transcription, translation, etc. This assay initially classified 12% of the detectable proteome as being differentially expressed in CADA-treated cells but at varying confidence levels ranging from as little as 1.25-fold change up to greater than twofold difference. We selected several candidate proteins based upon BD classification and a priori knowledge from literature for validation with classical immunoblots, flow cytometry, and cell-free *in vitro* translocation.

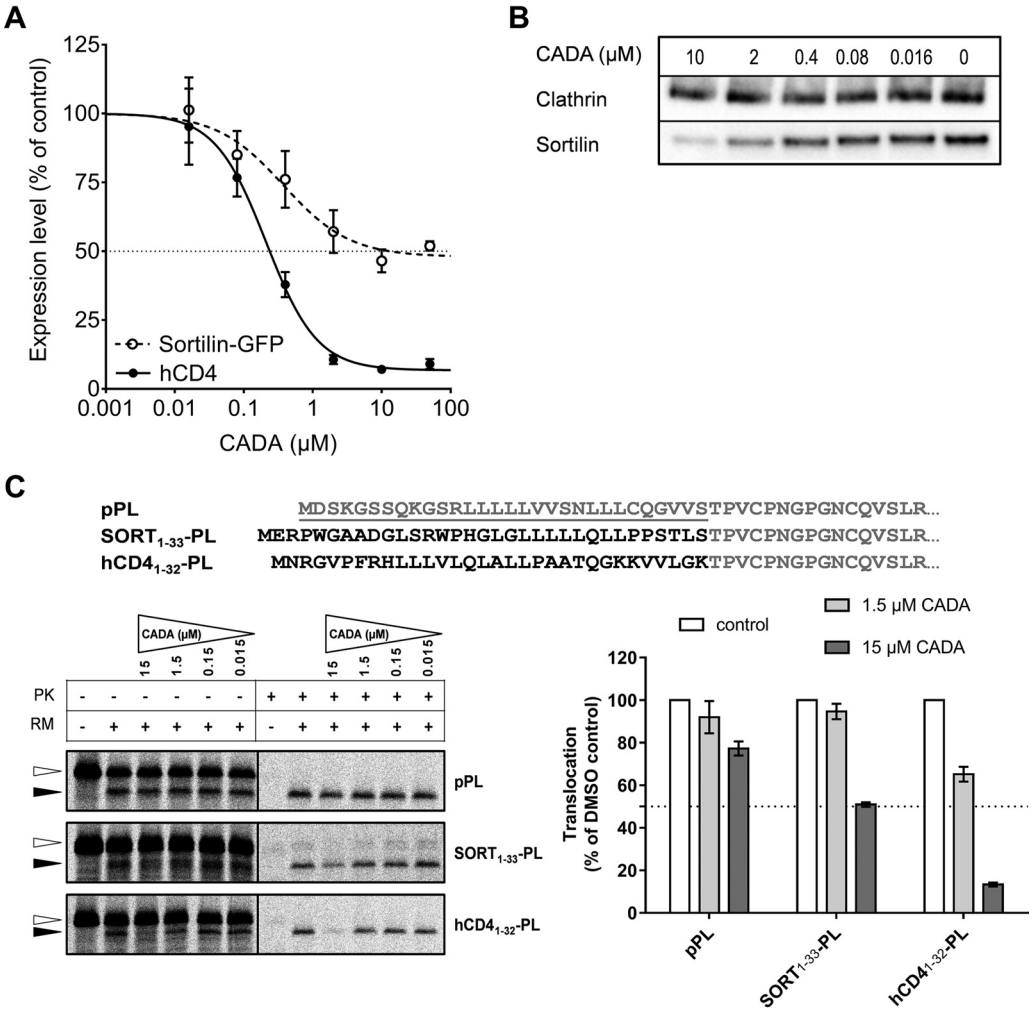

FIG. 5. **CADA partially down-modulates sortilin expression in a signal peptide-dependent way.** (*A*) HEK293T cells were cotransfected with human sortilin-GFP and human wild-type CD4 and were treated with the indicated amounts of CADA or 0.1% DMSO as a control. Sortilin and hCD4 expression were measured 48 h after transfection with flow cytometry (absolute IC_{50} values were 5.90 μM and 0.24 μM, respectively). Dotted line: sortilin-GFP; *solid line*: hCD4; mean ± S.E., $n = 3$. (*B*) After 72 h treatment of SUP-T1 cells with CADA, cells were lysed and sortilin was detected with Western blotting under nonreducing conditions. Detection was done with a rabbit antibody against human sortilin (clone EPR15010). (*C*) *Top panel* shows the N-terminal amino acid sequence of bovine preprolactin (pPL) and two signal peptide chimaera. The signal peptide of pPL (*underlined*, *gray*) was replaced with the sortilin or hCD4 signal peptide (*black*) for use in radiolabeled cell-free *in vitro* translation reactions. *Bottom left panel* shows representative autoradiogram of the *in vitro* translated and translocated pPL variants. In the presence of microsomes, the preprotein (*open arrowhead*) is translocated into the ER lumen and the signal peptide is cleaved off, resulting in a faster migrating mature protein (*black arrowhead*) that is protected inside rough microsome vesicles and thus protease K resistant. Signal intensities of the translocated protein fraction (*black arrowhead*) in protease K treated samples are shown in the *bottom right* graph. Bars are mean ± S.E.; $n \geq 3$.

Comparison between the PowerBlot analysis and the optimized validation immunoblots led us to conclude that use of the general multitarget PowerBlot array results in an elevated false positive rate. In the PowerBlot method, single samples were probed simultaneously with multiple antibodies, and identification of differentially migrating (and sometimes partially degraded) proteins based on expected molecular weight can therefore lead to misidentification and masking of signals through nonspecific interactions (for an example, see Fig. S1). The use of a single set of blotting conditions is also a compromise that may not allow successful detection of certain proteins in all sample types. For several of the PowerBlot hits, the difference between treated and untreated sample was classified as > twofold and was most likely overestimated, considering that no actual ratio could be calculated because of lack of signal in one of the matching samples (indicated with "n.v." in Table I). Nevertheless, the high-throughput immunoblotting PowerBlot screen is a well-suited proteomic technique not only to rapidly identify new targets for a drug but also to easily confirm potential hits since the PowerBlot antibodies are specified in the analysis and commercially available.

Our PowerBlot data indicated that some factors involved in cell cycle progression such as pRb2 (22), cyclin D3 (31), and c-Jun (25) are differentially expressed in CADA-treated cells. However, further analysis ruled out any inhibitory effect of CADA on cell cycle transition. These data are in line with previous observations that CADA has no antiproliferative effect on SUP-T1 cells. Cellular viability was not compromised by CADA and long-term CADA-treatment of T-cells was achieved, with preservation of hCD4 re-expression following workout (9). Lowering the amount of cell surface hCD4 by CADA treatment did not affect activation of the T cell receptor signaling pathway, probably because hCD4 is mainly important in the enhancement of T cell sensitivity to antigens (32, 33).

We have previously shown that the small molecule CADA down-modulates hCD4 surface expression by binding selectively to the hCD4 signal peptide, which inhibits the cotranslational translocation of hCD4 through the Sec61 channel (the translocon) (9). We therefore investigated whether other candidates of the PowerBlot proteome that contain a SP or signal anchor sequence were affected by CADA and confirmed that the ER-targeted protein sortilin was significantly down-modulated by CADA. Sortilin, also known as neurotensin receptor 3, is a 95 kDa type 1 transmembrane protein that belongs to the vacuolar protein sorting 10 protein domain receptor family. It is expressed in various cell types, (29) and intracellular sortilin is involved in protein sorting and targeting of ligands toward endosomes and lysosomes (30). Since both sortilin and hCD4 (which are down-modulated by CADA) depend on the ER secretory pathway for their cellular expression, future proteomic analysis should focus on the secretome and the plasma membrane fraction in order to fully examine the range of compound substrates. Although the list of detected secretory and membrane proteins was limited in our current study, the identification of only one additional CADA-substrate suggests that the compound may not induce a wide-ranging and global block on ER translocation.

Only a few other inhibitors of Sec61-mediated cotranslational translocation have been reported to date [for an overview, see the review by Kalies and Römisch (34)]. Most of these inhibitors interfere with a specific step in the translocation process and thus affect a wide spectrum of translocon substrates, often associated with cellular toxicity (35, 36). The fungal cyclic heptadepsipeptide HUN-7293 was originally identified as an inhibitor of vascular cell adhesion molecule 1 (VCAM-1) expression in endothelial cells (37, 38). Derivatives of this compound also act in a SP-dependent way, similar to CADA, but the precise mechanism of action and binding sites are likely different. The chemical structures show large differences and they affect the translocation of different target proteins. The derivative CAM741 inhibits the translocation of VCAM-1 and VEGF in a signal peptide-dependent way and interferes with the correct insertion of the VCAM-1 SP in the translocon (39–41). Another HUN-7293 derivative is cotransin, which inhibits the translocation of several secretory and membrane proteins in a signal peptide-dependent manner (42). It is suggested that cotransin binds to the Sec61 plug domain, near the lateral gate of the translocon channel, which prevents the inserted protein from reaching the lumen of the ER (43, 44), and may explain its broad substrate range. The selectivity of cotransin was recently addressed in a proteomic study (45), which revealed that the translocation of almost all secreted proteins was affected under saturating cotransin concentrations. However, the majority of integral membrane proteins were resistant to cotransin activity. Of note is that sortilin was identified in the limited list of cotransin-affected integral membrane proteins. It is known that translocating nascent proteins with different primary sequences place different demands on the transport machinery (46), and it seems that the conditions for the translocation of sortilin can be easily perturbed by different classes of small molecules that act within the ER translocon.

Our previous studies indicated that CADA inhibits passage of nascent hCD4 through the translocon by blocking reorientation of the SP within the channel (9). CADA binds directly to the hCD4 SP, apparently forming a discrete complex that is stabilized by electrostatic and other interactions between the drug and its target (47). Our working hypothesis is that CADA stabilizes an otherwise transitory folded conformation of the SP within the channel. As seen in Fig. 5*A*, translocation of hCD4 is not completely inhibited and the maximum down-modulation at high drug concentration is 87%. The IC_{50} value (concentration that produces 50% of total down-modulation) is 0.24 μM. Since the maximum effect of the compound on hCD4 is nearly 100%, this absolute IC_{50} value is almost the same as the relative IC_{50} value (0.21 μM), which is the concentration that produces 50% of maximal down-modulation (48). CADA is a much weaker inhibitor of sortilin translocation compared with hCD4. Fig. 5*A* shows that the maximal down-modulation of sortilin measured by flow cytometry is only about 50%, which is consistent with the results obtained through different techniques. According to our mechanistic hypothesis, CADA may also bind the sortilin SP in a folded conformation, but this complex less effectively inhibits protein translocation. The relative IC_{50} value (concentration that produces ca. 25% down-modulation of sortilin) of 0.38 μM shows that the CADA-sortilin SP complex is almost as stable as the CADA-hCD4 SP complex since this corresponds to the inflection point on the dose–response curve and to the dissociation constant, assuming that the complex has 1:1 stoichiometry. Further work with different SP mutants will help to identify which specific residues interact with CADA and refine our structural model for the SP-small molecule complex within the translocon. Ideally, identifying a primary sequence consensus motif in the SP required for CADA sensitivity would be a big step forward in understanding the molecular mechanism of action and the selectivity of CADA toward target SPs.

In conclusion, the present study suggested that CADA apparently has a low impact on the expression of almost 450 different cellular proteins. It also revealed that CADA inhibits sortilin translocation in an SP-dependent way but causes weaker down-modulation relative to hCD4. To further assess substrate selectivity, future studies on CADA should focus on the Sec61 secretory pathway and analyze a larger subset of secreted and membrane proteins, for example, with an unbiased technique such as stable isotope labeling with amino acids in cell culture-based mass spectrometry. So far, CADA's high selectivity for hCD4 down-modulation bodes well for its potential use as an alternative to anti-hCD4 antibodies in the treatment of numerous autoimmune diseases (49–52).

Acknowledgments—We thank B. Provinciael and A. Camps for excellent technical assistance and thank S. Carpentier for expert advice.

* The research was sponsored by the KU Leuven (GOA no. 10/014 and PF/10/018) and the FWO (no. G.485.08).

S This article contains supplemental material.

‖ To whom correspondence should be addressed: Herestraat 49, postbus 12134, 3000 Leuven, Belgium; Tel: +32-16-321925; Email: kurt.vermeire@kuleuven.be

¶ Both authors contributed equally.

REFERENCES

1. Lange, J. M., and Ananworanich, J. (2014) The discovery and development of antiretroviral agents. *Antivir. Ther.* **19,** 5–14
2. Vermeire, K., Zhang, Y., Princen, K., Hatse, S., Samala, M. F., Dey, K., Choi, H. J., Ahn, Y., Sodoma, A., Snoeck, R., Andrei, G., De Clercq, E., Bell, T. W., and Schols, D. (2002) CADA inhibits human immunodeficiency virus and human herpesvirus 7 replication by down-modulation of the cellular CD4 receptor. *Virology* **302,** 342–353
3. Vermeire, K., Bell, T. W., Choi, H. J., Jin, Q., Samala, M. F., Sodoma, A., De Clercq, E., and Schols, D. (2003) The Anti-HIV potency of cyclotriazadisulfonamide analogs is directly correlated with their ability to down-modulate the CD4 receptor. *Mol. Pharmacol.* **63,** 203–210
4. Vermeire, K., and Schols, D. (2003) Specific CD4 down-modulating compounds with potent anti-HIV activity. *J. Leukoc. Biol.* **74,** 667–675
5. Vermeire, K., Princen, K., Hatse, S., De Clercq, E., Dey, K., Bell, T. W., and Schols, D. (2004) CADA, a novel CD4-targeted HIV inhibitor, is synergistic with various anti-HIV drugs in vitro. *AIDS.* **18,** 2115–2125
6. Vermeire, K., Schols, D., and Bell, T. W. (2004) CD4 down-modulating compounds with potent anti-HIV activity. *Curr. Pharm. Des.* **10,** 1795–1803
7. Vermeire, K., Schols, D., and Bell, T. W. (2006) Inhibitors of HIV infection via the cellular CD4 receptor. *Curr. Med. Chem.* **13,** 731–743
8. Kwong, P. D., Wyatt, R., Robinson, J., Sweet, R. W., Sodroski, J., and Hendrickson, W. A. (1998) Structure of an HIV gp120 envelope glycoprotein in complex with the CD4 receptor and a neutralizing human antibody. *Nature.* **393,** 648–659
9. Vermeire, K., Bell, T. W., Van Puyenbroeck, V., Giraut, A., Noppen, S., Liekens, S., Schols, D., Hartmann, E., Kalies, K. U., and Marsh, M. (2014) Signal peptide-binding drug as a selective inhibitor of co-translational protein translocation. *PLoS Biol.* **12,** e1002011
10. Rapoport, T. A. (2007) Protein translocation across the eukaryotic endoplasmic reticulum and bacterial plasma membranes. *Nature.* **450,** 663–669
11. von Heijne, G. (1985) Signal sequences. The limits of variation. *J. Mol. Biol.* **184,** 99–105
12. Connolly, T., and Gilmore, R. (1986) Formation of a functional ribosome-membrane junction during translocation requires the participation of a GTP-binding protein. *J. Cell Biol.* **103,** 2253–2261
13. Erster, O., and Liscovitch, M. (2010) A modified inverse PCR procedure for insertion, deletion, or replacement of a DNA fragment in a target sequence and its application in the ligand interaction scan method for generation of ligand-regulated proteins. *Methods Mol. Biol.* **634,** 157–174
14. Emanuelsson, O., Brunak, S., von Heijne, G., and Nielsen, H. (2007) Locating proteins in the cell using TargetP, SignalP and related tools. *Nat. Protoc.* **2,** 953–971
15. Käll, L., Krogh, A., and Sonnhammer, E. L. (2004) A combined transmembrane topology and signal peptide prediction method. *J. Mol. Biol.* **338,** 1027–1036
16. Bijlmakers, M. J., and Marsh, M. (1999) Trafficking of an acylated cytosolic protein: Newly synthesized p56(lck) travels to the plasma membrane via the exocytic pathway. *J. Cell Biol.* **145,** 457–468
17. Pitcher, C., Höning, S., Fingerhut, A., Bowers, K., and Marsh, M. (1999) Cluster of differentiation antigen 4 (CD4) endocytosis and adaptor complex binding require activation of the CD4 endocytosis signal by serine phosphorylation. *Mol. Biol. Cell.* **10,** 677–691
18. Littman, D. R. (1987) The structure of the CD4 and CD8 genes. *Annu. Rev. Immunol.* **5,** 561–584
19. Liu, M. C., Akle, V., Zheng, W., Dave, J. R., Tortella, F. C., Hayes, R. L., and Wang, K. K. (2006) Comparing calpain- and caspase-3-mediated degradation patterns in traumatic brain injury by differential proteome analysis. *Biochem. J.* **394,** 715–725
20. Shen, J., Behrens, C., Wistuba, I. I., Feng, L., Lee, J. J., Hong, W. K., and Lotan, R. (2006) Identification and validation of differences in protein levels in normal, premalignant, and malignant lung cells and tissues using high-throughput Western Array and immunohistochemistry. *Cancer Res.* **66,** 11194–11206
21. Stanton, R. J., McSharry, B. P., Rickards, C. R., Wang, E. C., Tomasec, P., and Wilkinson, G. W. (2007) Cytomegalovirus destruction of focal adhesions revealed in a high-throughput Western blot analysis of cellular protein expression. *J. Virol.* **81,** 7860–7872
22. Sun, A., Bagella, L., Tutton, S., Romano, G., and Giordano, A. (2007) From G0 to S phase: A view of the roles played by the retinoblastoma (Rb) family members in the Rb-E2F pathway. *J. Cell. Biochem.* **102,** 1400–1404
23. Toogood, P. L., Harvey, P. J., Repine, J. T., Sheehan, D. J., VanderWel, S. N., Zhou, H., Keller, P. R., McNamara, D. J., Sherry, D., Zhu, T., Brodfuehrer, J., Choi, C., Barvian, M. R., and Fry, D. W. (2005) Discovery of a potent and selective inhibitor of cyclin-dependent kinase 4/6. *J. Med. Chem.* **48,** 2388–2406
24. Barber, E. K., Dasgupta, J. D., Schlossman, S. F., Trevillyan, J. M., and Rudd, C. E. (1989) The CD4 and CD8 antigens are coupled to a protein–tyrosine kinase (p56lck) that phosphorylates the CD3 complex. *Proc. Natl. Acad. Sci. U.S.A.* **86,** 3277–3281
25. König, R., and Zhou, W. (2004) Signal transduction in T helper cells: CD4 coreceptors exert complex regulatory effects on T cell activation and function. *Curr. Issues Mol. Biol.* **6,** 1–15
26. Di Bartolo, V., Mège, D., Germain, V., Pelosi, M., Dufour, E., Michel, F., Magistrelli, G., Isacchi, A., and Acuto, O. (1999) Tyrosine 319, a newly identified phosphorylation site of ZAP-70, plays a critical role in T cell antigen receptor signaling. *J. Biol. Chem.* **274,** 6285–6294
27. Balagopalan, L., Coussens, N. P., Sherman, E., Samelson, L. E., and Sommers, C. L. (2010) The LAT story: A tale of cooperativity, coordination, and choreography. *Cold Spring Harb. Perspect. Biol.* **2,** a005512
28. Abraham, R. T., and Weiss, A. (2004) Jurkat T cells and development of the T-cell receptor signalling paradigm. *Nat. Rev. Immunol.* **4,** 301–308
29. Reuter, E., Weber, J., Paterka, M., Ploen, R., Breiderhoff, T., van Horssen, J., Willnow, T. E., Siffrin, V., and Zipp, F. (2015) Role of sortilin in models of autoimmune neuroinflammation. *J. Immunol.* **195,** 5762–5769
30. Carlo, A. S., Nykjaer, A., and Willnow, T. E. (2014) Sorting receptor sortilin-a culprit in cardiovascular and neurological diseases. *J. Mol. Med.* **92,** 905–911
31. Boonen, G. J., van Oirschot, B. A., van Diepen, A., Mackus, W. J., Verdonck, L. F., Rijksen, G., and Medema, R. H. (1999) Cyclin D3 regulates proliferation and apoptosis of leukemic T cell lines. *J. Biol. Chem.* **274,** 34676–34682
32. Irvine, D. J., Purbhoo, M. A., Krogsgaard, M., and Davis, M. M. (2002) Direct observation of ligand recognition by T cells. *Nature* **419,** 845–849
33. Li, Q. J., Dinner, A. R., Qi, S., Irvine, D. J., Huppa, J. B., Davis, M. M., and Chakraborty, A. K. (2004) CD4 enhances T cell sensitivity to antigen by coordinating Lck accumulation at the immunological synapse. *Nat. Immunol.* **5,** 791–799

34. Kalies, K. U., and Römisch, K. (2015) Inhibitors of protein translocation across the ER membrane. *Traffic* **16,** 1027–1038
35. Liu, Y., Law, B. K., and Luesch, H. (2009) Apratoxin a reversibly inhibits the secretory pathway by preventing cotranslational translocation. *Mol. Pharmacol.* **76,** 91–104
36. Junne, T., Wong, J., Studer, C., Aust, T., Bauer, B. W., Beibel, M., Bhullar, B., Bruccoleri, R., Eichenberger, J., Estoppey, D., Hartmann, N., Knapp, B., Krastel, P., Melin, N., Oakeley, E. J., Oberer, L., Riedl, R., Roma, G., Schuierer, S., Petersen, F., Tallarico, J. A., Rapoport, T. A., Spiess, M., and Hoepfner, D. (2015) Decatransin, a new natural product inhibiting protein translocation at the Sec61/SecYEG translocon. *J. Cell Sci.* **128,** 1217–1229
37. Foster, C. A., Dreyfuss, M., Mandak, B., Meingassner, J. G., Naegeli, H. U., Nussbaumer, A., Oberer, L., Scheel, G., and Swoboda, E. M. (1994) Pharmacological modulation of endothelial cell-associated adhesion molecule expression: Implications for future treatment of dermatological diseases. *J. Dermatol.* **21,** 847–854
38. Boger, D. L., Chen, Y., and Foster, C. A. (2000) Synthesis and evaluation of aza HUN-7293. *Bioorg. Med. Chem. Lett.* **10,** 1741–1744
39. Besemer, J., Harant, H., Wang, S., Oberhauser, B., Marquardt, K., Foster, C. A., Schreiner, E. P., de Vries, J. E., Dascher-Nadel, C., and Lindley, I. J. (2005) Selective inhibition of cotranslational translocation of vascular cell adhesion molecule 1. *Nature* **436,** 290–293
40. Harant, H., Lettner, N., Hofer, L., Oberhauser, B., de Vries, J. E., and Lindley, I. J. (2006) The translocation inhibitor CAM741 interferes with vascular cell adhesion molecule 1 signal peptide insertion at the translocon. *J. Biol. Chem.* **281,** 30492–30502
41. Harant, H., Wolff, B., Schreiner, E. P., Oberhauser, B., Hofer, L., Lettner, N., Maier, S., de Vries, J. E., and Lindley, I. J. (2007) Inhibition of vascular endothelial growth factor cotranslational translocation by the cyclopeptolide CAM741. *Mol. Pharmacol.* **71,** 1657–1665
42. Garrison, J. L., Kunkel, E. J., Hegde, R. S., and Taunton, J. (2005) A substrate-specific inhibitor of protein translocation into the endoplasmic reticulum. *Nature* **436,** 285–289
43. MacKinnon, A. L., Garrison, J. L., Hegde, R. S., and Taunton, J. (2007) Photo-leucine incorporation reveals the target of a cyclodepsipeptide inhibitor of cotranslational translocation. *J. Am. Chem. Soc.* **129,** 14560–14561
44. Mackinnon, A. L., Paavilainen, V. O., Sharma, A., Hegde, R. S., and Taunton, J. (2014) An allosteric Sec61 inhibitor traps nascent transmembrane helices at the lateral gate. *Elife* **3,** e01483
45. Klein, W., Westendorf, C., Schmidt, A., Conill-Cortés, M., Rutz, C., Blohs, M., Beyermann, M., Protze, J., Krause, G., Krause, E., and Schülein, R. (2015) Defining a conformational consensus motif in cotransin-sensitive signal sequences: A proteomic and site-directed mutagenesis study. *PLoS ONE* **10,** e0120886
46. Zimmermann, R., Eyrisch, S., Ahmad, M., and Helms, V. (2011) Protein translocation across the ER membrane. *Biochim. Biophys. Acta* **1808,** 912–924
47. Chawla, R., Van Puyenbroeck, V., Pflug, N. C., Sama, A., Ali, R., Schols, D., Vermeire, K., and Bell, T. W. (2016) Tuning side arm electronics in unsymmetrical cyclotriazadisulfonamide (CADA) endoplasmic reticulum (ER) translocation inhibitors to improve their human cluster of differentiation 4 (CD4) receptor down-modulating potencies. *J. Med. Chem.* **59,** 2633–2647
48. Sebaugh, J. L. (2011) Guidelines for accurate EC50/IC50 estimation. *Pharm. Stat.* **10,** 128–134
49. Bartholomew, M., Brett, S., Barber, K., Rossman, C., Crowe, S., and Tite, J. (1995) Functional analysis of the effects of a fully humanized anti-CD4 antibody on resting and activated human T cells. *Immunology* **85,** 41–48
50. König, M., Rharbaoui, F., Aigner, S., Dälken, B., and Schüttrumpf, J. (2016) Tregalizumab—A monoclonal antibody to target regulatory T cells. *Front. Immunol.* **7,** 11
51. Choy, E. H., Connolly, D. J., Rapson, N., Jeal, S., Brown, J. C., Kingsley, G. H., Panayi, G. S., and Johnston, J. M. (2000) Pharmacokinetic, pharmacodynamic and clinical effects of a humanized IgG1 anti-CD4 monoclonal antibody in the peripheral blood and synovial fluid of rheumatoid arthritis patients. *Rheumatology* **39,** 1139–1146
52. Lorenz, H. M. (2003) T-cell-activation inhibitors in rheumatoid arthritis. *BioDrugs* **17,** 263–270